euspen's 22nd International Conference & Exhibition, Geneva, CH, May/June 2022
www.euspen.eu

Progress in nanometrology: reduction of measurement uncertainty of step height and etching depth calibration down to 0.3 nm

Gaoliang Dai, Xiukun Hu

Physikalisch-Technische Bundesanstalt (PTB), Bundesallee 100, 38116 Braunschweig, Germany
gaoliang.dai@ptb.de

Abstract
Metrological atomic force microscopes (Met. AFM) are one of the most widely used metrology tools for accurate and traceable calibrations of various nanoscale standards, which is a crucial task for developing innovative nanotechnologies. However, experimental studies show that the interferometers embedded in the Met. AFM suffer from high order nonlinearity error, which cannot be corrected by the conventional Heydemann method. To overcome this challenging issue, this paper introduces a new approach for correcting the high order nonlinearity errors by using external sensors/standards, which is feasible to correct the nonlinearity error down to 40 pm. Furthermore, the propagation of the (residual) nonlinearity error for the step height calibration is introduced. Finally, the metrology performance of the state-of-the-art Met. AFM at the PTB in the calibration of a highly demanding industrial sample is illustrated. The standard deviation of 6 sets of reproducible measurements reaches 0.02 nm and its expanded measurement uncertainty is estimated as 0.3 nm. This demonstrates a significant progress in dimensional nanometrology.

Dimensional nanometrology, traceable calibration, metrological atomic force microscopy, interferometry, nonlinearity correction, step height

1. Introduction

Accurate and traceable calibration of step height and/or etching depth of micro- and nanostructures is a fundamental task in nanometrology. Today, metrological atomic force microscopy (Met. AFM) is one of the most accurate methods for step height calibration, which offers a typical expanded measurement uncertainty of U of 1.0 ~ 2.0 nm ($k = 2$), as confirmed by the international comparison NANO2 [1]. However, there are increasing demands on the reduction of U to below 0.5 nm (0.3 nm desired) by some industrial sectors, for instance, the metrology of absolute feature heights of photomask structures and diffractive optical elements (DOEs) for the simulation and thus control of their (optical) functions.

To further improve the measurement accuracy of Met. AFM, recently a thorough study has been performed at the PTB, the national metrology institute of Germany. The study has focused on three key factors: (i) high-order nonlinearity errors of interferometers; (ii) ghost interference fringe present in the AFM optical detection system; and (iii) form deviation of measurement mirrors. Significant progress has been made, which lead to a reduction of measurement uncertainty for step height and etching depth calibrations from $U > 1.0$ nm to 0.3 nm.

This paper introduces the progress made at the PTB. Due to the length limit of the paper, only the study on the investigation and correction of the high-order nonlinearity errors of interferometers is focused on in this paper.

2. Principle of the Met. LR-AFM and its high-order interferometric nonlinearity error

Since 2004 a metrological large range atomic force microscopy (Met. LR-AFM) has been built up at the PTB [2], which is serving as one of the main workhorses for dimensional nanometrology at the PTB. The principle of the Met. LR-AFM is shown in figure 1(a). The sample (S) is mounted on a piezo stage (PZT-stage) which is in turn fixed to a motion platform (Mirror corner) of a high precision mechanical stage referred to as a Nanomeasuring machine (NMM) [3]. The mirror corner is moved by stacked mechanical x-, y- and z-stages, which offer a motion range of 25 mm, 25 mm and 5 mm, respectively. The 6 degree-of-freedoms (DOFs) motion of the mirror corners is measured by three interferometers and two autocollimators. In the setup, the AFM tip is located at the intersection point of three interferometer beams, thus, the design fully complies with the Abbe principle. The interferometers share one frequency stabilised He-Ne laser, whose optical frequency is calibrated by the iodine frequency stabilised laser at the PTB as 632 991 234 ± 5 fm, thus offering direct traceability for measuring the stage motions.

The Met.LR-AFM measures in the so-called scanning sample principle. During measurements, the sample is scanned in the xy-plane at the given speed, and is servo controlled along the z-axis to keep the AFM tip sample interaction constant. In such a way, the geometry of the nanostructure can be derived from the x-, y- and z-coordinates of the scanner, i.e. by the capacitive sensors embedded in the piezo stage and the interferometers of NMMs. Before the measurement, the capacitive sensor is traceably calibrated to the interferometers of the NMM.

The principle of the nanometric displacement measuring interferometer built-in in the NMM is shown in figure 1(b). It is a Michelson type homodyne interferometer with plane reference mirror (RM) and measurement mirror (MM). The incident laser beam is split into two beams with s- and p- polarisations by a polarising beam splitter (PBS) forming the reference and measurement beams, respectively. The reflected reference beam (s-polarisation) is turned into a circular polarisation beam by a quarter wave plate (QWP) whose fast axis is oriented at 45°. After being reflected by the RM and passed the QWP the 2nd time, the reference beam is turned into a p-polarisation and thus passes through the PBS. Similarly, after the measurement beam (p-polarisation) passed through a QWP, being reflected at MM and then passed the QWP the 2nd time, it is changed into s-polarisation and is reflected at the PBS, and thus recombined

with the reference beam forming the interference. The recombined beam is divided by a beam splitter (BS) into two detection beams, which after passing a pair of polarisers placed with an angle of 45° to each other, generates a pair of 90° phase-shifted signal S_{cos} and S_{sin}. Such a signal pair ideally forms a circular Lissajous figure where the phase shift (φ) of the interferometer can be determined. The displacement of the MM can be calculated as:

$$L = \frac{\lambda}{2n}(m + \frac{\varphi}{2\pi}\varphi) \quad (1)$$

where, λ is the vacuum wavelength of the applied laser source; n is the air refractive index; m is the measured integer interference fringes; and φ is the measured phase indicating the fractional interference fringe.

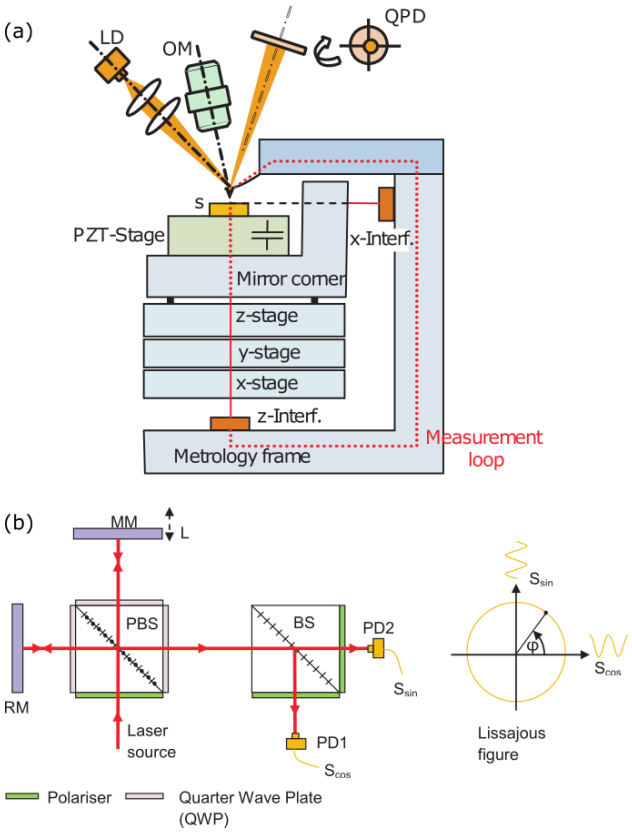

Figure 1. Schematic diagram showing the measurement principle of (a) the Met. LR-AFM; and (b) the homodyne interferometer embedded for measuring the displacements of the scanner motion.

Ideally, the homodyne interferometer provides a pair of electrical signals (u_1, u_2) with zero offset, identical amplitude, and exact 90° phase difference. However, polarization mixing, laser power offsets, laser beam misalignment, imperfection of electronic processing and error motion of stage will cause the Lissajous trajectory of two phase-quadrature signals to be distorted from the ideal circle, consequently leading to the well-known issue of nonlinearity errors of interferometers. In our previous study, two distorted phase-quadrature signals (u_1^d, u_2^d) obtained by photo detectors were expressed as following [4]:

$$u_1^d = u_1 + p$$
$$u_2^d = \frac{1}{r}(u_2 \cos\alpha - u_1 \sin\alpha) + q \quad (2)$$

The Lissajous trajectory of (u_1^d, u_2^d) is a least squares fit to an ellipse for the calculation of fitting parameters of p, q, r and α, based on which the ideal vector (u_1, u_2) can be recovered from the measured vector (u_1^d, u_2^d). By applying this method, also known as the Heydemann correction method [5], the nonlinearity error was effectively corrected with a residual amplitude below 0.3 nm in our previous metrological AFM type Veritekt C [4].

However, in experimental measurements we found that the Heydemann correction method is insufficient to correct the interferometric nonlinearity error in the Met. LR-AFM. To illustrate this problem, figure 2(a) plots the measured Lissajous trajectory of the z-interferometer of the Met. LR-AFM, shown as measured raw signals (in black), Heydemann corrected signals (in red) and an ideally fitted circle (in blue). At first sight these signals seem to have a very good fit to the circular shape. However, a zoom-in view in figure 2(b) indicates a very strong shape deviation of the interferometer signals. It indicates that the measured phase-quadrature signal (u_1^d, u_2^d) can no more be described by equation 2, leading to the failure of the Heydemann correction method for this device. Consequently, it results in a kind of high order nonlinearity error. For this given example, the amplitude of such high order nonlinearity was measured > 1 nm, becoming one of the most significant error sources for the Met. LR-AFM for performing sub-nm accurate nanometrology.

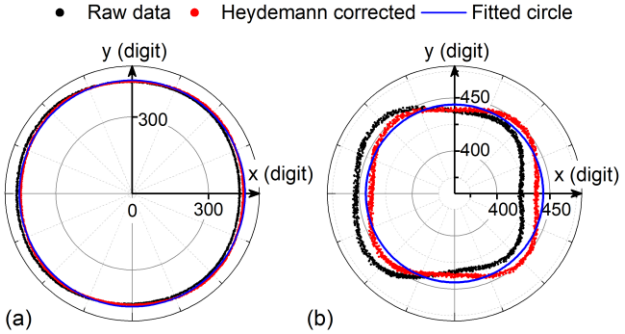

Figure 2. Lissajous trajectory of the z-interferometer of the Met. LR-AFM shown as (a) raw data, Heydemann corrected data and a fitted ideal circle; and (b) a zoom-in view showing the shape deviation of interferometer signals.

3. Correction of high order nonlinearity error

Generally speaking, there are two categories of methods for the correction of interferometric nonlinearity error. One is the theoretical correction method based on the model of the distorted interferometric signal, such as equation 2 applied in the Heydemann correction. Its advantage is that no external standards/sensors are needed for the correction. However, the disadvantage is that the correction will fail (significantly) if the model deviates from the real situation, as shown in figure 2. The other method is the correction method using external sensors/standards. It has advantages that it needs no theoretical model of the distorted interferometric signal, thus better applicable for correcting high order nonlinearity errors. However, external sensors/standards are needed for the correction whose quality will impact the correction performance, which will be demonstrated later in the paper.

Due to the difficulty to (exactly) model the distorted interferometric signal for correcting high order nonlinearity error, we applied the external sensors/standards method in this research. Using this method, the selection and application of the external sensor/standard is key important. It should have high quality and be convenient for usage. In this paper, we use two kinds of sensors/standards: one is the embedded capacitive sensors in the piezo stage; the other is the use of a kind of physical artefacts (i.e. a good quality samples or material measures). Our experiment shows that both of them are capable of (effectively) correcting the high order nonlinearity error. However, due to the limit of the paper length, only the correction method by applying the physical artefacts is detailed below.

The results of the correction method based on a physical artefact — a glass flat is shown in figure 3. In the correction, the glass flat is intentionally mounted in the Met. LR-AFM with a slight tilting angle (about 0.6 °) in the xz plane, where the x-axis is fast scan axis. After an AFM topography image of the sample surface is obtained as shown in figure 3(a), it is fitted to a planar surface using a least squares fit. The residual form error between the measured and fitted surface topography is plotted in figure 3(b). A periodical disturbance can easily be seen, which may be attributed to (i) the nonlinearity error of the z-interferometer; and/or (ii) a (rather unlikely) form error of the sample surface. In the data evaluation, we extract a segment of data with a height change Δz of 633 nm, which (exactly) equals the wavelength of the laser source, λ_{laser}, as shown in figure 3(c). It can be seen that there are 8 periods of disturbance in the measured topography, which indicates the existence of 4th order nonlinearity error. Note that one interference fringe in a single pass interference indicates a length of λ_{laser} /2.

The nonlinearity error of the z-interferometer can be easily determined by performing a Fourier Transformation (FT) of the extracted profile marked in figure 3(c). The FT result is shown in figure 3(d). It contains frequency components which have frequencies $f = 2n/\lambda_{laser}$ (where n = 1, 2, 3, 4, …), as marked in red. It can be regarded as the nonlinearity error of the z-interferometer, as will be discussed in detail later. The remaining frequency components, i.e., those which have frequencies other than $f = 2n/\lambda_{laser}$ are shown in black. They can be attributed to e.g. (i) surface topography of the sample; (ii) the measurement errors e.g. noise. After performing an inverse FT on the red marked frequency components while set the amplitude of black marked components to 0, a nonlinearity error curve of the z-interferometer can be obtained, as indicated by the red line in figure 3(c).

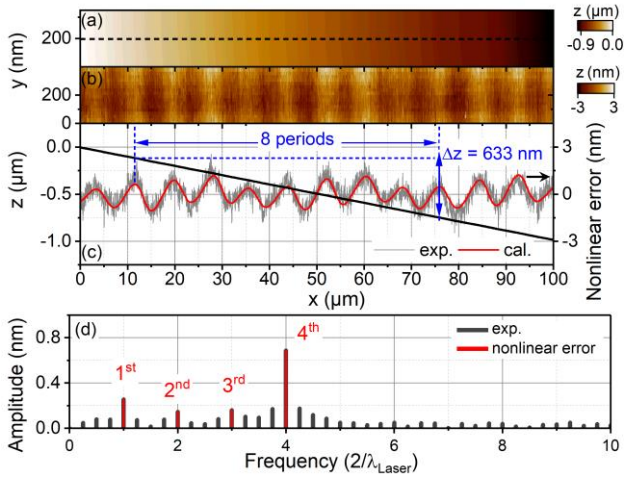

Figure 3. Correction of high order nonlinearity error of z-interferometer using a flat surface. (a) Measured raw data of a flat surface. (b) Flat surface after applying a planar fitting. (c) Measured (black) and calculated (red) high order nonlinearity error of z-interferometer. (d) Fourier Transformation results, where the harmonic nonlinearity error of the z-interferometer is shown in red;

Using the method described above, however, there is a fundamental question: "how does the surface quality of the physical artefact impact the nonlinearity correction?". It is due to the fact that the sample surface may also contain frequency components which overlap with that of the nonlinearity error, leading to correction error. Our answer to this question is that such errors do exist, however, because only the frequency components of surface which exactly overlap with the periodical frequencies of nonlinearity errors will contribute, it is not significant. To experimentally confirm this issue, nonlinearity error of the z-interferometer characterised by using five different sample surfaces (made of silicon and glass), which have a roughness *R*a of about 2 nm, is compared in figure 4(a). The result shows a good agreement with each other. The averaged result of five nonlinearity curves of figure 4(a) is shown in figure 4 (b). The standard deviation of five measurements is also shown in figure 4(b) in purple colour, which has an amplitude mostly below 0.1 nm (about 0.2 nm at the maximum), showing the effectiveness of the developed method.

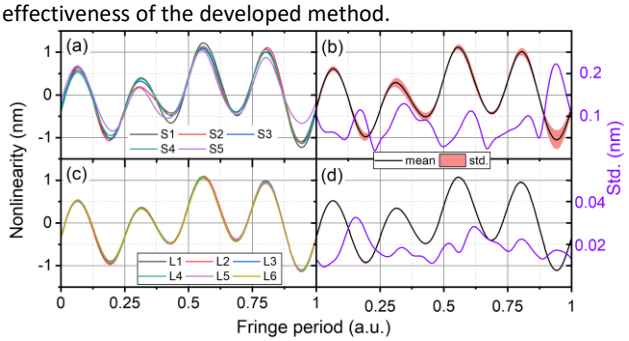

Figure 4. Experiment result of high order nonlinearity correction using a flat surface shown as (a) the nonlinearity curves characterised by five normal glass and silicon sample surface with a *R*a of about 2 nm; (b) the averaged nonlinearity curve of the curves shown in (a) and their standard deviation curve;(c) the nonlinearity curves characterised by a ultra-fine crystal silicon sample surface with a *R*a of < 0.3 nm; (d) the averaged nonlinearity curve of the curves shown in (c) and their standard deviation curve

To further investigate the surface quality of the sample on the nonlinearity correction performance, we had also characterised the nonlinearity error of the z-interferometer using an ultra-fine crystal silicon surface which has a surface roughness *R*a of less than 0.3 nm. The measurements were performed on five different locations of the same surface with different measurement conditions (i.e., different AFM heads, tips, and scan parameters etc.). The obtained nonlinearity error curves are shown in figure 4(c-d). More stable nonlinearity curves with a standard deviation below 0.04 nm have been obtained.

After the averaged nonlinearity curve has been calculated as shown in figure 4(b) or 4(d), they can be applied as a look-up table to correct the nonlinearity error of the interferometer. To illustrate the performance of such a correction, a measurement of the optical flat used in figure 3 is repeated after the nonlinearity correction method has been applied. The resulted topography is shown in figure 5 after removing its fit plane. It can be seen that the periodical disturbance shown in figure 3 has been fully removed, confirming the effectiveness of the proposed nonlinearity correction method.

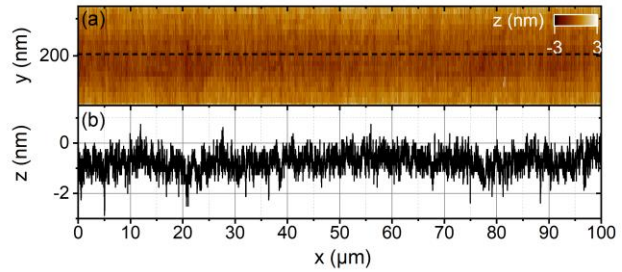

Figure 5. Measurement results of a flat surface after the correction of high order nonlinearity errors

4. Error propagation of (residual) nonlinearity in step height and etching depth calibration

It has been detailed in Section 3 that high order nonlinearity error of interferometers can be well characterised and corrected. For high precision dimensional nanometrology, however, the residual nonlinearity error even after the correction is still one of the dominant error sources. Consequently, the error propagation of (residual) nonlinearity in step height and etching

depth calibration is crucial. However, such an analysis is not so straight-forward because the nonlinearity error is a kind of nonlinear function of the coordinate of the measured pixels.

To have an intuitive illustration on how the nonlinearity error impacts the step height and etch depth calibration, a specially designed experiment is performed. In this measurement, as shown in figure 6(a), a grating sample is well aligned along its fast scan axis (i.e., x-axis) without tilting angle, while it is slightly titled with an angle (measured as 0.44 °) along its slow scan axis (i.e., y-axis). The measured AFM image is depicted in figure 6(a) as the raw data. According to ISO5436, the height of the grating feature is evaluated line by line, where the height offset between the (selected segments of) top and bottom profiles are evaluated as the feature height. For simplicity, it is denoted as:

$$h = z_t(x,y) - z_b(x,y) \quad (3)$$

where $z_t(x,y)$ and $z_b(x,y)$ indicate the z coordinate of the top and bottom profiles, respectively. The propagated error contribution of nonlinearity error on the feature height metrology is:

$$u = N_z(z_t(x,y)) - N_z(z_b(x,y)) \quad (4)$$

where $N_z(z)$ indicate the nonlinearity error of the z-interferometer at the position z. Using equation (4), it is thus possible to set up a numerical simulation model to investigate the error propagation using e.g., the Monto-Carlo simulation method.

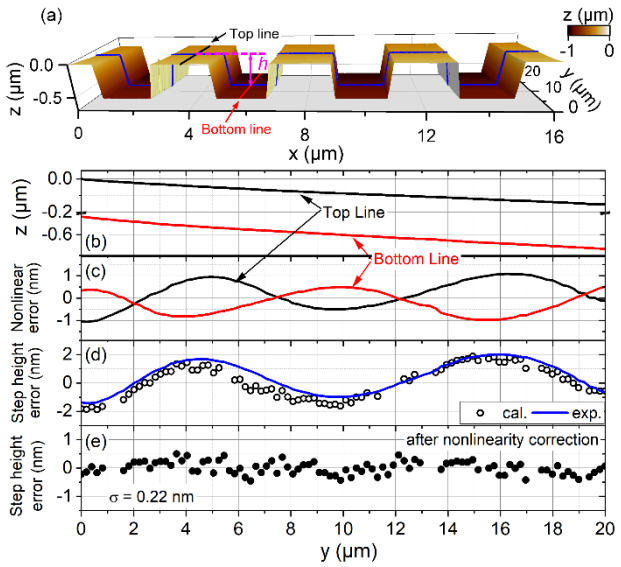

Figure 6. Measurement results of a study investigating the propagation of the nonlinearity error in step height calibration. See text for details

In this experiment, as the sample is perfectly aligned along the x-axis, we can simplify the investigation by observing the nonlinearity error at a top profile (at $x = x_t$) and a bottom profile (at $x = x_b$) along the y-axis, as indicated in figure 6(a) by the black and red lines, respectively. Due to the inclination of the sample along the y-axis, its z-coordinate $z_t(x_t,y)$ and $z_b(x_b,y)$ varies with respect to y, as shown in figure 6(b). The changed z-coordinates introduce different nonlinearity errors at the top and bottom profiles, as shown in figure 6(c) when the proposed correction of high order nonlinearity error is disabled. It finally leads to an error contribution in the height measurement, shown as a solid curve in blue in figure 6(d). The measured feature height variation is shown in circular marks. A very good agreement can be seen between the simulated and experimental results. It indicates that the nonlinearity error is the dominant error source which leads to the variation of the measured feature height.

For a comparison, the variation of the measured feature height after applying the nonlinearity error correction method is shown in figure 6(e). It can be seen the measurement results become much more stable owing to the reduced nonlinearity error.

4. Performance of step height and etch depth calibration after improvement

To finally demonstrate the performance of the state-of-the-art Met. LR-AFM after improvement, the calibration results of a highly demanding industrial sample are plotted in figure 7. In this calibration, the sample is measured at 25 different locations. Six sets of measurements are repeated, performed with three different AFM heads (AFM1, AFM3 and AFM4) and six different AFM probes (3 with type PPP_NCLR and 3 with type PPP-NCHR, all from Nanosensors®). It can be seen that the results have excellent reproducibility. The standard deviation of the mean feature height of 6 sets of measurements reaches 0.02 nm, indicating the measurement stability and reproducibility of the metrology tool. The standard deviation of all 150 results (i.e., 6 sets × 25 results per set) is 0.08 nm, indicating both the reproducibility of the metrology tool and the sample uniformity. The preliminary measurement uncertainty of this calibration is estimated as 0.3 nm, which is a significant improvement compared to the previous result (about 1.0 ~ 2.0 nm).

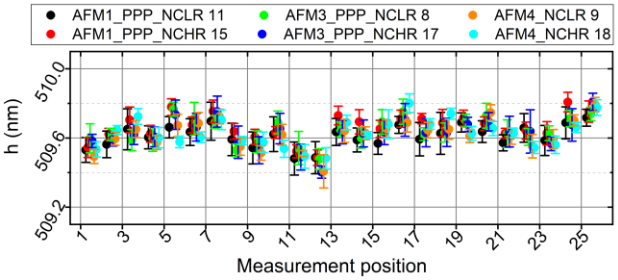

Figure 7. Metrology performance of the state-of-the-art Met. LR-AFM after improvement shown as the calibration result of a highly demanding industrial sample

In summary, this paper introduces a challenging problem concerning the high order nonlinearity error of interferometers in the Met. LR-AFM of the PTB, where the well-known Heydemann correction method fails to properly correct. To solve this problem, a new correction method by using external sensors/standards has been developed. The experimental result show that it can effectively reduce the nonlinearity error down to 0.04 nm. Furthermore, the propagation of the (residual) nonlinearity error for the step height calibration is introduced. Finally, the metrology performance of the Met. LR-AFM in the calibration of a highly demanding industrial sample is demonstrated: the standard deviation of 6 sets of reproducible measurements reaches 0.02 nm. This shows a significant progress for accurate and traceable dimensional nanometrology.

Note that, It is the nonlinearity error of the z-interferometer that is focused on in this paper. It is due to the fact that the performance of the z-interferometer is much more critical than the x- and y- interferometers in step height and etch depth calibrations. However, the method can be expanded for the interferometers of the other axes as well.

References

[1] Koenders L et al. 2003 Metrologia 40 Tech. Suppl. 04001
[2] Dai G et al 2004 Rev. Sci. Instrum. 75 962–9
[3] Manske E et al 2007 Meas. Sci. Technol. 18 520
[4] Dai G et al 2004 Meas. Sci. Technol. 15 444–50
[5] Heydemann P., 1981 Appl. Opt. 20, 3382